APPLYING THE VOLUME AVERAGING THEORY TO OPEN-CELL METAL FOAM IN NATURAL CONVECTION/RADIATION

De Schampheleire S.*, De Kerpel K., Huisseune H., De Jaeger P., Ameel B. and De Paepe M.
*Author for correspondence
Department of Flow, Heat and Combustion Mechanics,
Ghent University,
9000 Ghent,
Belgium,
E-mail: Sven.DeSchampheleire@ugent.be

ABSTRACT

Heat sinks made out of open-cell aluminium foam are investigated numerically in natural convection. Results derived from a 2D numerical model are compared to results for in-house experiments. Different foam heights are studied. The numerical model is based on the volume averaging theory. The aluminium foam that is used has 10 pores per linear inch and a porosity of 93%. The temperature of the substrate was varied between 55°C and 95°C. The geometry used in the numerical model replicates the experimental test rig as well as possible. A discussion of the determination of the closure terms is given.

If only convective heat transfer is taken into account in the numerical model, the relative differences between the numerical and experimental results are smaller than 29% for all foam heights studied. However, when the influence of radiation is included in the numerical model, it is shown that the numerical results differ less than 9% with the experimental ones. This validates the choice of closure terms used in the model and this shows that it is necessary to properly model radiative heat transfer in numerical models of open-cell aluminium foam in natural convection.

INTRODUCTION

Open-cell metal foams are looked at as a new fin materials. It has very high porosities (>90%), which makes the material quite light. The foam has thin struts, creating many tortuous pathways and keeping the boundary layers thin which leads to an increase in the interstitial heat transfer. Due to the high surface-to-volume ratio of metal foams and the deformability in three dimensions, a foam heat sink can be made compact and robust.

The foams studied in this work are manufactured in-house by an investment casting technique, replicating an organic preform. A detailed description of the production process can be found in De Jaeger [1]. The nomenclature for open-cell aluminium foam (struts, nodes, pores and cells) is illustrated in Figure 1. Manufacturers often characterize the foam by providing the PPI value (Pores Per linear Inch) and porosity ϕ [1].
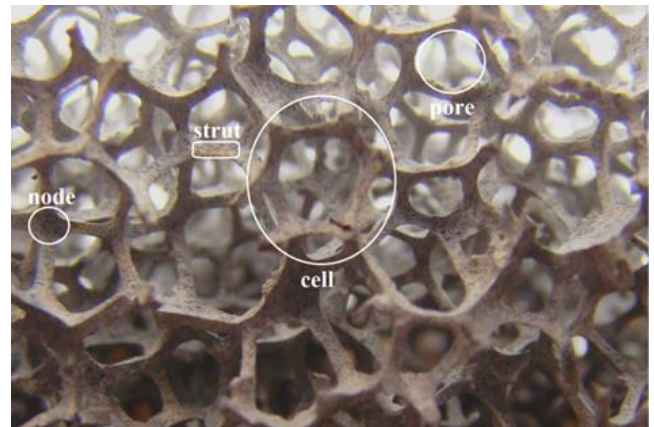

Figure 1 Nomenclature of open-cell metal foam

NOMENCLATURE

$\dot{Q}$	[W]	electric power supply
A	[m²]	area
c_p	[J/kgK]	specific heat capacity
h	[W/m²K]	heat transfer coefficient
k	[W/mK]	thermal conductivity
P	[N/m³]	pressure
Re	[-]	Reynolds number
T	[K]	temperature
v	[m/s]	velocity

Special Characters

β	[1/m]	inertial coefficient
ε	[-]	emissivity
κ	[m²]	permeability
μ	[Pa.s]	dynamic viscosity
ρ	[kg/m³]	density
σ	[W/m²K⁴]	Stefan-Boltzmann constant
ϕ	[-]	porosity
Δ	[-]	difference

Subscripts

conv	convective
d	dispersion
e	effective
env	environment
exp	experimental
f	fluid

fs	interfacial
num	numeric
r	radiative
s	solid
s	substrate

Superscripts

| i | intrinsic |

Abbreviations

PPI	Pores Per linear Inch
PUC	Periodic Unit Cell
TCR	Thermal Contact Resistance

OPEN-CELL METAL FOAM IN NATURAL CONVECTION

Many parameters influence natural convection in metal foam. De Schampheleire et al. [2] listed all important parameters for this case: foam material, foam height, geometrical characteristics of the foam, the length-to-width ratio of the heat sink substrate, inclination angle under which the heat sink is positioned, temperature difference between the environment and the substrate, radiative heat transfer contribution, contact resistance between substrate and foam (dependent on the bonding method), construction details of the test rig and the dimensions of the enclosure surrounding the heat sink. Furthermore, these parameters tend to interact which each other, making the analysis of buoyancy driven heat transfer a complex task. Available literature on natural convection in open-cell metal foam is limited. Only some of the listed parameters have been studied and reported. In the following, an overview is given of the experimental and numerical work done in natural convection.

Experimentally, Bhattacharya and Mahajan [3] studied the influence of pore density and porosity. The authors found that the heat transfer rate increases with a decrease in porosity or increase in metal content. When the porosity is constant, higher pore densities results in a lower heat transfer rate. The influence of the heat sink inclination angle is studied by Qu et al. [4] for copper foam. The inclination angle was varied in steps of 15° from vertical to horizontal orientation. The effect on the Nusselt number was only 6%. Finally, De Schampheleire et al. [2] analysed the influence of different foam heights, pore densities and bonding technologies for a heat sink with a length-to-width ratio of 10. The foam height was varied between 12 and 40 mm, the pore density was 10 and 20 PPI. Two bonding techniques were tested (epoxy and brazing) to investigate contact resistance. They reported that the strongest influence on heat transfer rate is attributed to a variation in sample height.

The question is now which parameters should be examined in order to achieve accurate prediction of buoyancy driven heat transfer. To be able to study the effect of all these parameters within an acceptable time frame, some work is also done to study foam numerically. To capture the details of the flow through the foam, microscopic models are used. However, due to time and resource constraints the computational domain is mostly restricted to a limited number of numerical cells. To simulate the complete heat sink, macroscopic models based on the volume averaging theory (VAT) are preferred. Such models also allow optimization of the heat sink for a certain application. In natural convection, Phanikumar and Mahajan [5] and Zhao et al. [6] used VAT to model heat transfer and fluid flow in open-cell foams. Both authors used a 2D thermal non-equilibrium model. Phanikumar and Mahajan [5] compared their results with the experimental data from Bhattacharya and Mahajan [3]. They reported a good match (<15% difference) between both results. On the other hand, Zhao et al. [6] reported deviations between their experimental and numerical results up to 28%. Phanikumar and Mahajan [5] and Zhao et al. [6] do not mention the possible influence of radiative heat transfer on the simulated results, but neglected the radiative heat transfer altogether.

However, it is expected that radiative heat exchange with the surrounding (external radiation) is not negligible in natural convection. For foam heat sinks, to the authors' knowledge the work by De Schampheleire et al. [7] is the only one which investigated the influence of radiation experimentally for a heat sink with dimensions of 102x165 mm². Painting the foam black resulted in a heat transfer rate increase up to 11%. This proves that external radiation is not negligible in natural convection

In contrast to foam heat sinks, a lot of research is available on radiation in pin fin heat sinks. Sahray et al. [8] found that for a given fin height, the relative contribution of radiation is usually higher for both loose (12 mm free space in between the pins) and dense (6 mm free space) sinks compared to the intermediate sinks. This was explained by the fact that loose surfaces have a higher exposure to the surroundings, while in a dense sink the inter-fin spacing behave like cavities, and the 'effective emissivity' is much higher than the nominal one. For pin fins, radiative contributions up to 45% of the total heat transfer rate were found. Foams can be categorized as dense sinks as the cells are smaller than 6 mm diameter. Sparrow and Vemuri [9] studied the effect of orientation and radiation on natural convection/radiation heat transfer in pin fins. The fractional contributions of radiation to the combined-mode heat transfer were generally in the 25-40% range, with the larger contributions occurring for the smaller temperature differences between substrate and environment.

The review above clearly indicates the need for a thermal non-equilibrium macroscopic model, which allows accurate predictions of natural convection in open-cell foam heat sinks. A higher accuracy than the models listed above is required when optimization of the foamed heat sinks is aimed for. That is why in this work a 2D macroscopic model for natural convection in open-cell metal foam is developed. The accurateness of the model is verified by comparing numerical predictions with in-house measurements on heat sinks with different foam heights [2]. The influence of thermal radiation is investigated and discussed. It will be shown that these effects are not negligible and in fact necessary to close the gap with the experimental results. Finally, a sensitivity analysis is performed, in order to determine which parameters are the most important in metal foam heat sinks under natural convection.

METHOD
Comparison with Experiments

The experimental setup and measurements used in this work is described in De Schampheleire et al. [2], see also Figure 2. The tested foam heat sink has a fixed length-to-width ratio of 10. The substrate on which the foam is placed measures 254 x 25.4

x 4 mm³. Both the metal foam sample and the substrate are made of AL1050 aluminium alloy. Between the substrate and the electrical main heater, two copper plates with a thickness of 2.5 mm are mounted to make the heat flow uniform over the substrate. Grooves are machined in the copper plates to hold 6 K-type thermocouples. Below the copper plates, the main heater is placed. To enhance the thermal contact between the copper plates and the aluminium substrate, as well as between the copper plates and the heater, thermal paste is used. The thicknesses of the thermal paste layer are measured after each set of experiments and the sum was found to be at most 1.5 mm for the cases studied. The power dissipated by the main heater is determined by measuring its voltage and current.

To minimize the heat losses to the environment, three guard heaters are installed (see Figure 2). Similar to the main heater, the guard heaters are also accompanied with a copper plate and three mounted thermocouples. The heaters are controlled to obtain a constant temperature at the boundary. For the guard heaters, the bottom copper plate measures 254 x 25.4 x 5 mm³ and both side copper plates measure 254 x 50.8 x 5 mm³. The heat losses in these directions were estimated using a 2D finite element simulation and were found to be smaller than 0.2% of the total heat transfer rate. This is because the complete test assembly is mounted in high quality insulation material with a thermal conductivity of 0.023 W/mK. The overall relative uncertainty on the total heat transfer rate dissipated by the main heater was always smaller than 3%.

The foam studied here has a pore density of 10 PPI and a porosity of 93.3%. The temperature of the substrate was varied between 55°C and 95°C. Four foam heights were tested: 40 mm, 25.4 mm, 18 mm and 12 mm. An uncertainty analysis was performed. All thermocouples were calibrated and the uncertainty was determined to be 0.1K. The heat transfer rate $\dot{Q}_{exp}$ together with the temperature difference between the substrate and the environment is reported in Figure 6 to 9 for different foam heights.

Numerical Method

A general treatment on the up-scaling of transport phenomena in porous media, via volume averaging, is presented in the work of Whitaker [10]. Basically the microscopic equations (continuity, momentum and the energy equations for both solid and fluid phase) are averaged over a Periodic Unit Cell (PUC). After averaging over this PUC, the macroscopic model for the foam reads as Eq. (1) to (4). It is clear that these equations are similar to the microscopic Navier-Stokes equations: the local variables are replaced by the phase averaged variables and some closure terms appear. These closure terms represent the influence of the unresolved phenomena on the macroscopic flow. De Jaeger [1] modelled these closure terms based on macroscopic geometric properties of the foam and the Reynolds number for forced convection in metal foams. The same closure models will be used in this study. The resulting equations allow predicting
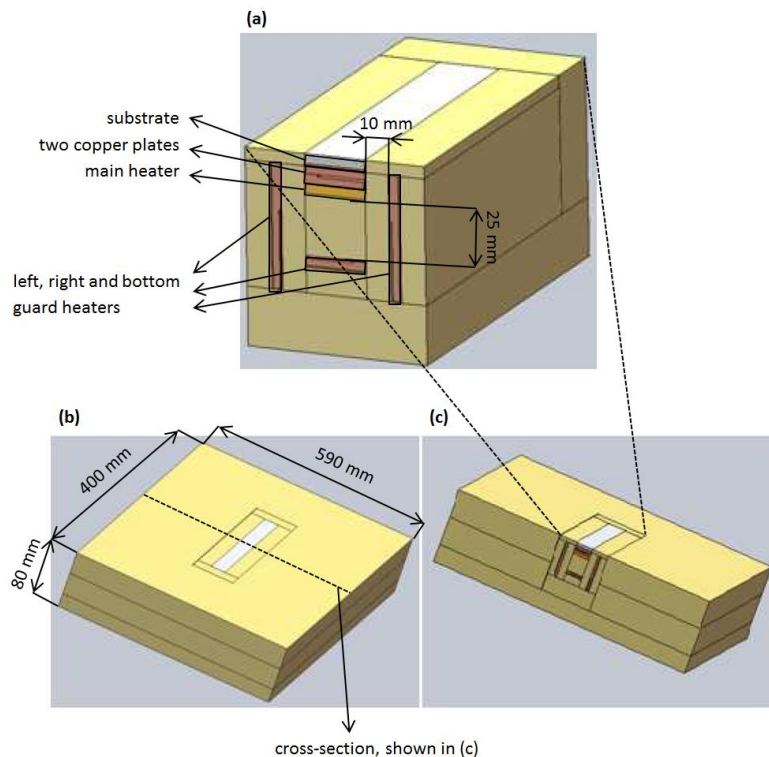

Figure 2 Illustration of the experimental test rig. (a) shows the cross section of the heater assembly, and (b) and (c) show the surrounding insulation.

the macroscopic behaviour of the metal foam, without having to resolve all the microscopic details of the flow. This significantly reduces the computational time.

$$\nabla \cdot \langle \vec{v} \rangle^i = 0 \qquad (1)$$

$$\rho \frac{\partial \langle \vec{v} \rangle^i}{\partial t} + \rho \langle \vec{v} \rangle^i \cdot \nabla \langle \vec{v} \rangle^i = -\nabla \langle P \rangle^i + \mu_e \nabla^2 \langle \vec{v} \rangle^i + \rho \vec{g}$$
$$-\mu \kappa^{-1} \cdot \langle \vec{v} \rangle^i - \rho \beta |\langle \vec{v} \rangle^i| \langle \vec{v} \rangle^i \qquad (2)$$

$$\phi (\rho c_p)_f \frac{\partial \langle T_f \rangle^i}{\partial t} + \phi (\rho c_p)_f \langle \vec{v} \rangle^i \cdot \nabla \langle T_f \rangle^i = \nabla \cdot k_{f,e} \cdot \nabla \langle T_f \rangle^i$$
$$+ h_{fs} \sigma_0 (\langle T_s \rangle^i - \langle T_f \rangle^i) \qquad (3)$$

$$(1-\phi)(\rho c_p)_s \frac{\partial \langle T_s \rangle^i}{\partial t} = \nabla \cdot k_{s,e} \cdot \nabla \langle T_s \rangle^i$$
$$- h_{fs} \sigma_0 (\langle T_s \rangle^i - \langle T_f \rangle^i) \qquad (4)$$

Closure term modeling and determination of effective properties

Whitaker [10] showed that closing the volume averaged momentum equation results in the Darcy-Forchheimer-Brinkman equation. This is used to determine the closure terms permeability κ and inertial loss coefficient β for the momentum equation. By doing this, one can recognize that the integrals for κ and β are respectively the viscous and the pressure force which act on the fluid-solid interface. These forces are calculated on a PUC through an implicit LES in De Jaeger et al. [11]. They are dependent on the Reynolds number. For high and low Reynolds numbers, the permeability is quasi-constant. For Re > 115, the corresponding permeability equals $4.43 \cdot 10^{-7}$ m². While for the lowest Re (Re < 10-1), the permeability is found to be $1.255 \cdot 10^{-6}$ m². For the inertial coefficient and Reynolds numbers higher than 10, the inertial loss factor is nearly constant and 86.7 m⁻¹. In case of no recirculation (Re < 10), the inertial loss factor decreases with increasing Re. This means that the pressure force increases at a lower rate than the averaged kinetic energy in the flow domain. From the moment that the recirculation regions in the wakes downstream the struts appear (Re > 10), the increment of pressure force and average kinetic energy is equal. This is characterized by a nearly constant inertial loss factor.

The momentum dispersion is described by the effective viscosity μ_e. Numerical and experimental studies have indicated that in the limit of φ→1, effective and molecular viscosity should become equal and that for a decreasing porosity, μ_e/μ increases. For highly porous media, a recent study of Nabovati and Amon [12] gave additional confirmation that the widely accepted model $\mu_e/\mu = 1/\phi$ is valid. In this work, the effective viscosity follows this model.

The effective fluid thermal conductivity can be expressed as a sum of the thermal dispersion k_d and the fluid conductivity k_f. In natural convection, the dispersion term is negligible [13]. In its turn, the fluid conductivity is function of the tortuosity of the foam. The tortuosity is an estimate of the ratio of the effective pathway to the chord length between two points in the fluid (or solid) phase. Brun [14] reported a value of 0.98 for the fluid tortuosity for Nickel and ERG aluminium Duocel® foams. As ERG foams strongly resemble the foams used in this work, the expression for the effective fluid conductivity now reads: $k_{f,e} = 0.98 \phi k_f$.

In this work, the effective solid thermal conductivity $k_{s,e}$ is determined by solving the continuum-scaled heat conduction in the solid phase of a PUC, like done in De Jaeger [1]. Based on this work, $k_{s,e}$ is taken equal to 5.4 W/mK for the studied 10 PPI foam. The obtained value matches with the experimental results published by Schmierer and Razini [15] in vacuum conditions for aluminium foams with porosities ranging from 88.6% to 96.2%.

Finally, the interstitial convective heat transfer coefficient h_{fs} is determined with a correlation for natural convection around a heated horizontal cylinder. The correlation is recommended by Raithby and Hollands [16]. The correlation is a function of the Rayleigh number and uses an average strut diameter as characteristic length. In this work $4 \cdot (1-\phi)/\sigma_0$ is used as average strut diameter, taking into account the thicker nodes at the end of the strut.

Implementation of the geometric model

The geometry is shown in Figure 3 and replicates the experimental test rig shown in Figure 2 as well as possible. Due to the large length-to-width ratio of the tested heat sinks (10/1), a two-dimensional numerical approach is justified. The dashed area in Figure 3 is fluid domain, while the domain indicated with 'MF' (metal foam) is the porous zone. Below the porous zone, an aluminium substrate with a thickness of 4 mm is modelled, together with a copper plate with a total thickness of 5 mm. Underneath the copper plate, a 1.5 mm thick layer of thermal paste is added. This one thick layer accounts for the contributions of the different layers of thermal paste used in the experiments. For the sake of simplicity the copper plates attached to the guard heaters and the physical thickness of the main and guard heaters are neglected in the simulated geometry. The main and guard heaters are indicated with a green line in Figure 3. The thermal conductivity of AL1050, copper, the thermal paste and the insulation material is taken resp. 220 W/mK, 387.6 W/mK, 0.8 W/mK and 0.023 W/mK respectively.
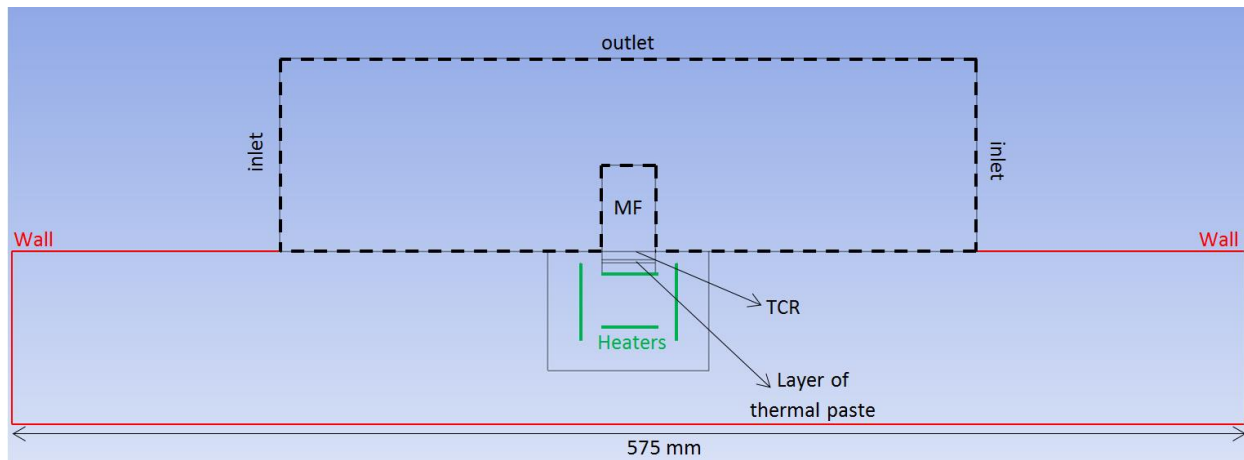
Figure 3 Implementation of the geometry in the CFD package

To limit the number of fluid cells in the computational domain, only 150 mm of fluid domain on the left and right of the metal foam is considered. The height of the fluid domain is always 2.25 times the foam height. So for a foam height of 40 mm, the total fluid height is 90 mm. The fluid and solid geometry is discretized with 2 control volumes per mm. Other finer meshes are tested as well as other heights and widths for the fluid domain, with no significant differences for either the flow or energy fields.

For the open boundaries where the air enters the simulated domain, the ambient pressure was used as a stagnation boundary condition with the incoming mass having the temperature of the environment. The static pressure was assumed to be equal to the pressure of the surrounding atmosphere where the air leaves the simulated domain. The temperature of the main heater and guard heaters were fixed at T_s. The temperature of the outer insulation is fixed at T_{env}. The heat transfer rate $\dot{Q}$ is calculated and compared to the experimental results.

Also the thermal contact resistance (TCR) between the metal foam and the substrate is taken into account. The TCR causes a temperature jump at the interface between the substrate and the foam. This interface is indicated in Figure 3. De Jaeger et al. [17] studied four different bonding techniques to connect the foam to the substrate and determined the respective thermal contact resistance. In the validation experiment used in this work, the foam is brazed to the substrate. For a brazed contact, De Jaeger et al. [17] reported a TCR of $0.7*10^{-3}$ m²K/W. The TCR between the substrate and respectively the solid and fluid phase is implemented in the numerical simulation.

The pressure correction is obtained via the SIMPLE algorithm, since steady-state calculations are performed. The convective terms are discretized through a second order upwind scheme, while diffusion terms are second order accurate central differenced. The spatial discretization of the pressure term is body forced weighted. The density is calculated according to the incompressible ideal gas law. As no Boussinesq model is used, the operating density at the environment temperature has to be specified. The macroscopic equations (Eq. (1)-(4)) are solved in the regions of the computational domain indicated as porous medium: 'MF' in Figure 3. For the porous zone, each cell holds information for both the fluid and the solid domain of the foam. In the other fluid regions, the microscopic transport equations are solved. The conservation equations in the fluid part, both for the porous zone as well as for the outer fluid region, are solved simultaneously as one field. The coupling between the solid and fluid phase energy transfer is achieved by computing the interstitial heat transfer rate at the fictional air/foam interface and the solid and fluid phase temperature from previous iteration.

Iterative convergence is verified by noting that the residuals drop below 10^{-11} for continuity and below 10^{-12} for velocity and energy fields, within 75,000 iterations and less than 2 hours of computing time per set point (12 dual hex core Xeon X5690 3.46Ghz processors – on board memory: 96 GB DDR3-1333 MHz RAM). The resulting energy balance closes within 0.01%
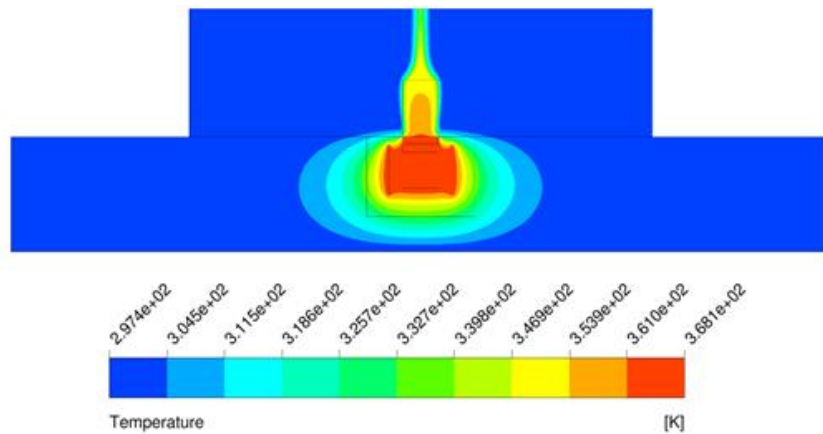
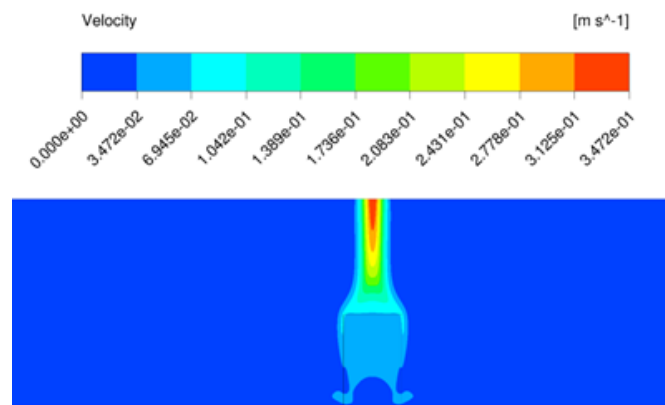**Figure 4** Temperature contours for the 40 mm foam samples (highest temperature difference: 70.6K)

Figure 5 Velocity contours for the 40 mm foam sample (highest temperature difference: 70.6K)

RESULTS AND DISCUSSION
Results

The numerical and pure convective results for all tested foam heights are summarized and compared with the experimental results in Figures 6 to 9. The 2D numerical results in Watt per meter are rescaled for the 254-mm-long heat sink. For all foam heights, heat transfer rate predicted by the numerical model is lower than the experimentally obtained value. The relative difference between the experimental and numerical results is on average 20% and does not depend much on the foam height. It will be shown that this under prediction is largely due to the neglected effect of external radiation. Figure 4 shows the fluid temperature of the foam together with the temperatures of the insulation material for the highest foam sample and temperature difference tested, resp. 40 mm and 70.6K. The simulations are performed for convective heat transfer only.

It is clear that the guard heaters are working as expected (no temperature difference between the guard heaters and the main heater) and the main heater is sending a one dimensional flux to the foam substrate. Because the length-to-width ratio is large, a single chimney type flow pattern is observed. Figure 5 displays the velocity contours around the foam material. Due to the low permeability of the foam and high inertial coefficient, it is quite difficult for the surrounding air to penetrate into the foam.

Phanikumar and Mahajan [5] observed a similar behaviour. Therefore, the fluid and solid temperature in the foam material is high as only at the foam boundaries some air is able to penetrate into the foam. Only at these boundaries the foam cooled slightly. The solid temperature of the foam is displayed in Figure 10. The decrease of the solid temperature over the foam domain is not very large. This means that the fin efficiency, also called foam efficiency, is quite high. This is expected for buoyancy driven flow [18]. For this 40 mm foam sample and the highest investigated temperature difference, the temperature decrease from bottom to top of the solid foam matrix is smaller than 13K.

The highest local convection coefficients are at the two top ends (left and right top end). There the lowest foam temperatures are observed. Above the heat sink, a hot air plume is observed. In that plume, the maximum velocity is observed. However, the average velocity in the foam domain for the highest foam sample and for the highest temperature difference tested is 0.04 m/s.
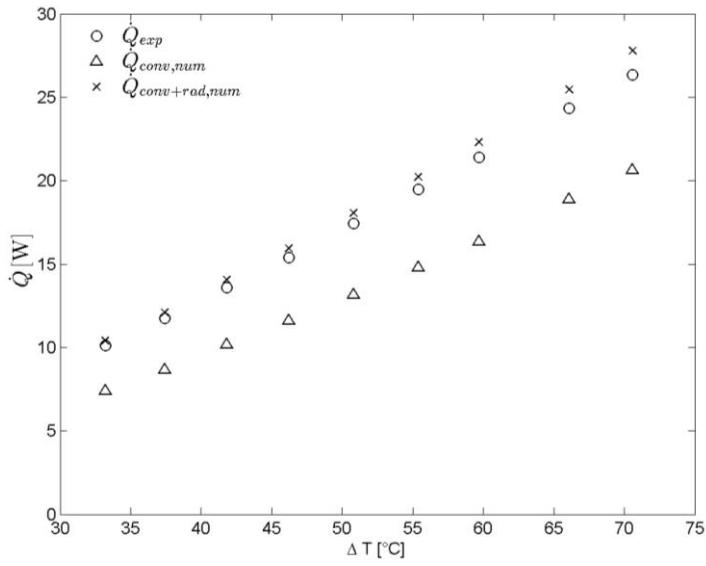
Figure 6 Comparison of the numerical results with the experimental ones and effect of radiative heat transfer: 40 mm sample
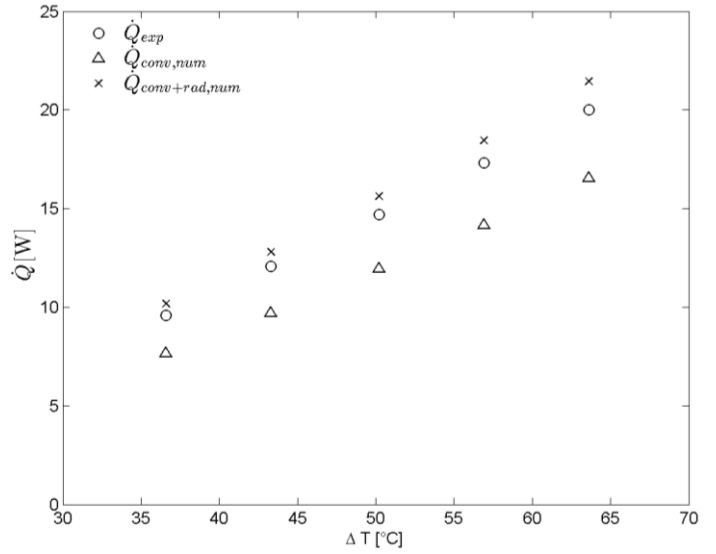

Figure 7 Comparison of the numerical results with the experimental ones and effect of radiative heat transfer: 25.4 mm sample
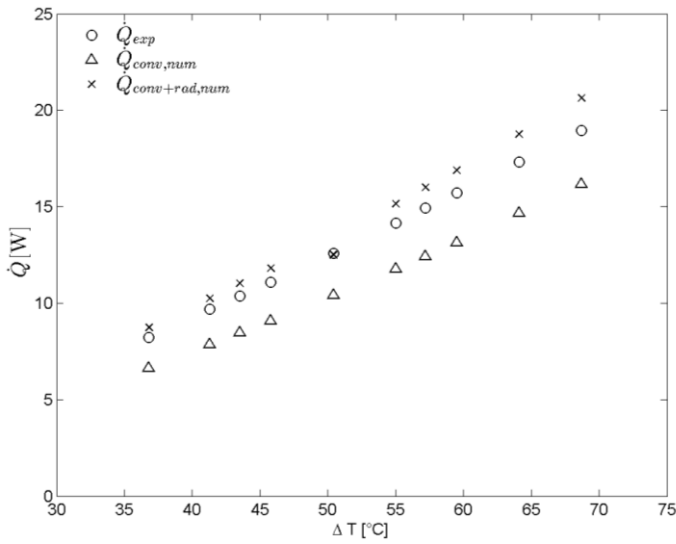

Figure 8 Comparison of the numerical results with the experimental ones and effect of radiative heat transfer: 18 mm sample
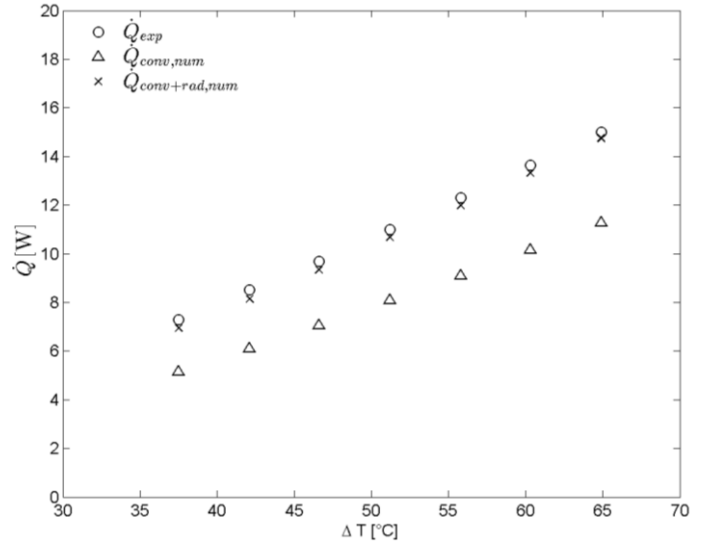

Figure 9 Comparison of the numerical results with the experimental ones and effect of radiative heat transfer: 12 mm sample

Impact of Radiation

One of the most important assumptions made in the simulation results shown in the previous section is neglecting the effect of radiation, as done in Refs. [5] and [6]. In order to determine whether this assumption is acceptable the effect of external radiation is estimated through the simplified Stefan-Boltzmann law (Eq. (5)).

$$\dot{Q}_{rad} = \varepsilon\sigma A(T_{hot}^4 - T_{env}^4) \tag{5}$$

In the above equation the view factors to the surroundings are neglected. Furthermore, ε is the emissivity of the foam material, A is the external surface area exposed to the surroundings, T_{env} is the temperature of the surroundings and T_{hot} is the temperature of the foam at the surface of the foam exposed to the surroundings. This T_{hot} is calculated for each set point as an average temperature over the surface.

The emissivity depends on the surface finish of the foam (gray, white, shiny…), as well as on the geometrical characteristics. An emissivity value of 55% is used in this work [19]. The resulting $\dot{Q}_{rad}$ yields an indication of the influence of external radiation for these heat sinks. The results for the different studied foam heights are reported in Figures 6 to 9. Generally, the simulations now slightly over predict the experimental data, expect for the lowest foam sample (see Figure 9). The influence of radiation is the highest for the largest foam height, up to 30% of the total heat transfer rate. This is well within the expected range of 25-40% as reported in open literature [9]. The trends also show a decrease of the relative influence of radiation to the experimental values when the temperature difference increases. The same trends were observed by Sparrow and Vemuri [9]. The results of our study clearly show that for natural convection in open-cell metal foam the radiative share in the total heat transfer cannot be neglected.

In Figure 10, the influence of the radiative heat transfer is shown graphically for the largest foam height and highest temperature difference simulated. Three heat transfer rates were reported: the experimental $\dot{Q}_{exp}$, the pure convective $\dot{Q}_{conv,num}$ and the combined convection/radiation $\dot{Q}_{conv+rad,num}$. For the highest foam, the differences between the combined heat transfer rate and the experimental one are very small: lower than 5% for each temperature difference simulated. For the other foam heights, the difference between $\dot{Q}_{exp}$ and $\dot{Q}_{conv+rad,num}$ stays below 9%. From Figures 6 to 9, it can be seen that the numerical results for pure convection show a similar trend when compared to the experimental results.

CONCLUSIONS

In this work a macroscopic model is developed which allows simulation natural convection in heat sinks with open-cell aluminium foam as an extended surface are studied in natural convection with air as working medium. Experiments of 10 PPI brazed aluminium foam with a porosity of 93.3% is compared with a 2D numerical model based on the volume averaging technique. In total four foam heights are studied: 40 mm, 25.4
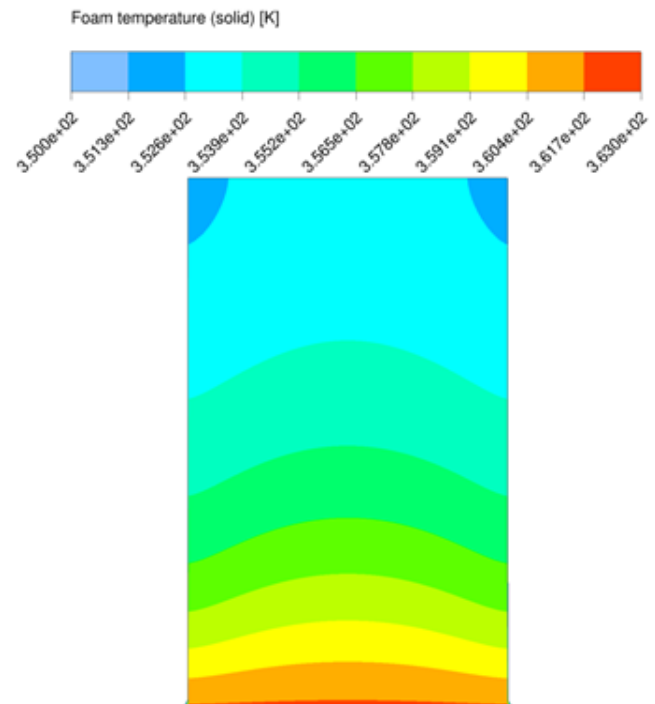

Figure 10 Illustration of the solid temperature field for the highest foam sample tested (temperature difference: 70.6K)

mm, 18 mm and 12 mm. When radiative heat transfer is not taken into account, the relative differences between the numerical results and the experiments are always smaller than 29%. When radiation is included in the numerical model, by applying the Stefan-Boltzmann equation, the numerical results differ less than 9% from the experimental results. This shows that the radiative heat transfer to the surroundings has to be taken into account for natural convection in open-cell foam even at low temperatures.

REFERENCES

[1] De Jaeger P., Thermal and hydraulic characterisation and modelling of open-cell aluminium foam. PhD thesis, Ghent University, Ghent, Belgium, 2012. ISBN: 978-90-8578-566-8.

[2] De Schampheleire S., De Jaeger P., Reynders R., De Kerpel K., Ameel B., T'Joen C., Huisseune H., Lecompte S., De Paepe M., Experimental study of buoyancy-driven flow in open-cell aluminium foam heat sinks, *Applied Thermal Engineering*, Vol. 59, 2013, pp. 30-40.

[3] Bhattacharya A., Mahajan R.L., Metal foam and finned metal foam heat sinks for electronics cooling in buoyancy-induced convection, *Journal of Electronic Packaging*, Vol. 128, 2006, pp. 259-266.

[4] Qu Z., Wang T., Tao W., Lu T., Experimental study of air natural convection on metallic foam-sintered plate, *International Journal of Heat and Fluid Flow*, Vol. 38, 2012, pp. 126-132.

[5] Phanikumar M.S., Mahajan R.L., Non-darcy natural convection in metal foams with open cells, *International Journal of Heat and Mass Transfer*, Vol. 45, 2002, pp. 3781-3793.

[6] Zhao C.Y., Lu T.J., Hodson H.P., Natural convection in metal foams with open cells, *International Journal of Heat and Mass Transfer*, Vol. 48, 2005, pp. 2452-2463.

[7] De Schampheleire S., De Kerpel K., Kennof G., Pirmez P., Huisseune H., De Paepe M., Comparison of aluminium foam finned

heat sinks and effect of painting and orientation in buoyancy-driven convection, in: proceedings of the 15th International Heat Transfer Conference, IHTC-15, August 10-15, 2014, Kyoto, Japan, p. 10. Paper number: IHTC15-8865.

[8] Sahray D., Shmueli H., Ziskind G., Letan R., Study and optimization of horizontal-base pin-fin heat sinks in natural convection and radiation, *Journal of Heat Transfer*, Vol. 132, 2010, pp. 012503-1 – 012503-13.

[9] Sparrow E.M., Vemuri S.B., Orientation effects on natural convection/radiation heat transfer from pin-fin arrays, *International Journal of Heat and Mass Transfer*, Vol. 29, 1986, pp. 359-368.

[10] Whitaker S., The method of volume averaging, Springer Science & Business Media, 1998, Heidelberg, Germany, pp. 219.

[11] De Jaeger P., De Schampheleire S., T'Joen C., Huisseune H., Ameel B., De Paepe M., Closure term modeling of the volume averaged transport equations for open cell foam, in: proceedings of the 9th International Conference on Heat Transfer, Fluid Mechanics and Thermodynamics (HEFAT2012), 16-18 July 2012, Malta.

[12] A. Nabovati, C. Amon, Hydrodynamic boundary condition at open-porous interface: a pore-level lattice Boltzmann study, *Transport in Porous Media*, 2012, pp. 1-13.

[13] Kaviany M., Principles of heat transfer in porous media, Springer, Heidelberg, Germany, 1995.

[14] Brun E., De l'imagerie 3D des structures à l'étude des mécanismes de transport en milieu cellularies, PhD thesis, Aix Marseille Université, France, 2009.

[15] Schmierer E.N., Razani A., Self-consistent open-celled metal foam model for thermal applications, *Journal of Heat Transfer-Transactions of the ASME*, Vol. 128, 2006, pp. 1194-1203.

[16] Nellis G., Klein S., Heat transfer, Cambridge university press, 2009, Cambridge, United Kingdom, p. 1143

[17] De Jaeger P., T'Joen C., Huisseune H., Ameel B., De Schampheleire S., De Paepe M., Assessing the influence of four bonding methods on the thermal contact resistance of open-cell aluminum foam, *International Journal of Heat and Mass Transfer*, Vol. 55, 2012, pp. 6200-6210.

[18] Ghosh I., Heat transfer correlation for high-porosity open-cell foam, *International Journal of Heat and Mass Transfer*, Vol. 52, 2009, pp. 1488-1494.

[19] Zhao C.Y., Tassou S.A., Lu T.J., Analytical considerations of thermal radiation in cellular metal foams with open cells, *International Journal of Heat and Mass Transfer*, Vol. 51, 2008, pp. 929-940.